

# Effect of normal current corrections on the vortex dynamics in type-II superconductors

P. Lipavský,<sup>1</sup> A. Elmurodov,<sup>1</sup> Pei-Jen Lin,<sup>2</sup> P. Matlock,<sup>3</sup> and G. R. Berdiyrov<sup>4</sup>

<sup>1</sup>*Faculty of Mathematics and Physics, Charles University, Ke Karlovu 3, 12116 Prague 2, Czech Republic*

<sup>2</sup>*Department of Physics, Old Dominion University, 4600 Elkhorn Avenue, Norfolk, Virginia 23529, USA*

<sup>3</sup>*Research Department, Universal Analytics Inc., Airdrie, AB, Canada*

<sup>4</sup>*Departement Fysica, Universiteit Antwerpen, Groenenborgerlaan 171, B-2020 Antwerpen, Belgium*

(Received 4 April 2012; revised manuscript received 23 August 2012; published 15 October 2012)

Within the time-dependent Ginzburg-Landau theory we discuss the effect of nonmagnetic interactions between the normal current and supercurrent in the presence of electric and magnetic fields. The correction due to the current-current interactions is shown to have a transient character so that it contributes only when a system evolves. Numerical studies for thin current-carrying superconducting strips with no magnetic feedback show that the effect of the normal current corrections is more pronounced in the resistive state where fast-moving kinematic vortices are formed. Simulations also reveal that the largest contribution due to current-current interactions appears near the sample edges, where the vortices reach their maximal velocity.

DOI: [10.1103/PhysRevB.86.144516](https://doi.org/10.1103/PhysRevB.86.144516)

PACS number(s): 74.78.Na, 73.23.-b

## I. INTRODUCTION

Although the time-dependent Ginzburg-Landau (TDGL) theory is justified only for slowly evolving systems, it provides qualitatively correct description of dynamic phenomena, such as ultrafast propagation of magnetic flux dendrites,<sup>1,2</sup> fast-moving kinematic vortices,<sup>3,4</sup> or accelerated vortex motion present during vortex-antivortex annihilation.<sup>5</sup> Of course, in these fast processes the quasiparticles cannot achieve a local equilibrium distribution; nonequilibrium corrections to TDGL theory become important. This was demonstrated by Vodolazov and Peeters<sup>6</sup> who found a large deformation of the gap profile at the phase-slip center in the case of a slow relaxation of quasiparticles. They assumed isotropic distribution of quasiparticles (valid in the dirty limit) and carefully treated the energy distribution using two coupled kinetic equations for longitudinal and transverse branches. Their approach applies for a finite value of the gap, the time derivative of which acts as a force driving quasiparticles out of equilibrium.

Here we discuss a complementary correction, valid in the pure limit, which takes into account a direction-dependent perturbation of the quasiparticle momentum distribution, which appears when the normal current is created in the system. The correction to the TDGL equation will be proportional to the scalar product of the normal current and the supercurrent.<sup>7</sup>

### A. Normal current in a superconductor

Superconductors with freely moving Abrikosov vortices or propagating dendrites have a finite resistivity and an electric field  $\mathbf{E}'$  thus develops in them as the current is driven through. This electric field generates a normal current

$$\mathbf{J}_N = \sigma_N \mathbf{E}', \quad (1)$$

which is in addition to the supercurrent  $\mathbf{J}_S$ . In the TDGL theory these two currents interact only indirectly via the magnetic field. The absence of any direct interaction between the normal current and supercurrent in this theory is not disturbing, because it is in agreement with an intuitive picture based on the two-fluid model of a superconductor: Taking the condensate

as an autonomous fluid one expects it not to interact with the underlying crystal including its normal electrons.

The absence of interaction between normal current and supercurrent is also supported by microscopic theories based on the dirty limit.<sup>8-11</sup> These approaches, however, cannot be used to discuss the current-current interaction. To obtain practical equations, authors employ the isotropic approximation<sup>6,9,11</sup> in some cases making the additional assumption of local equilibrium.<sup>8</sup> The isotropic distribution corresponds to zero normal current, therefore any effect of the normal current on formation of the superconducting gap is lost by this approximation.

The effect of the normal current on the gap has been derived in Ref. 7 from the Thouless criterion<sup>12</sup> adapted to nonequilibrium Green functions. This approach was applied to far-infrared conductivity of the Abrikosov vortex lattice by some authors of the current work,<sup>13</sup> which resulted in better agreement with a recent experiment<sup>14</sup> than the standard TDGL theory. Since the microscopic derivation is lengthy and technically demanding, in the Appendix we provide a simple derivation of the interaction of the condensate with the normal current, using purely phenomenological arguments.

### B. Plan of paper

The paper is organized as follows. In Sec. II we introduce the floating-kernel approximation which enables one to include the interaction between the normal current and supercurrent into the TDGL theory. In Sec. III we show that this correction is of transient nature being zero in any steady regime. To this end in Sec. III A we perform a gauge transformation to express the interaction of the normal current and supercurrent in terms of time derivative of the vector and scalar potential. Consequently, one can describe this correction in terms of effective magnetic and electric fields as shown in Sec. III B. In Sec. IV we apply our theory to the phase-slip regime in thin superconducting strips with negligible magnetic feedback. We express the TDGL formulation in terms of dimensionless quantities, which are used in numerical simulations; results of these simulations are used to demonstrate how the current-current interaction influences fast kinematic vortices in the

phase-slip regime. Our findings are summarized in Sec. V. In the Appendix we indicate why the TDGL theory violates the longitudinal  $f$ -sum rule and show that solving this problem with an intuitive two-fluid correction leads directly to the floating-kernel approximation.

## II. FLOATING-KERNEL APPROXIMATION

Here we write down a closed set of equations forming the *floating-kernel approximation*. This theory becomes identical to the TDGL theory in the coordinate system floating with normal electrons, as the normal current vanishes in this reference frame.

### A. Order parameter

In the presence of normal current the time evolution of the order parameter is described by<sup>7,13</sup>

$$\begin{aligned} & \frac{1}{2m^*} \left( -i\hbar\nabla - \frac{e^*}{c}\mathbf{A} - \frac{m^*}{en}\mathbf{J}_N \right)^2 \psi + \alpha\psi + \beta|\psi|^2\psi \\ &= -\frac{\Gamma}{\sqrt{1+C^2|\psi|^2}} \left( \frac{\partial}{\partial t} + \frac{i}{\hbar}e^*\phi + \frac{C^2}{2}\frac{\partial|\psi|^2}{\partial t} \right) \psi. \end{aligned} \quad (2)$$

The right-hand side has been derived by Kramer and Watts-Tobin three decades ago.<sup>9,15</sup> The  $\alpha$  and  $\beta$  terms are a standard part of the Ginzburg-Landau theory. The kinetic energy term on the left-hand side has been obtained only recently.<sup>7</sup> In the case of clean superconductors, the effective mass of a Cooper pair is  $m^* = 2m$  and its charge is twice the electron charge;  $e^* = 2e$ . In the Appendix this normal current correction is deduced from the longitudinal  $f$ -sum rule. The standard TDGL equation<sup>9</sup> can be obtained by setting  $\mathbf{J}_N = 0$ .

Away from the critical line, when  $C^2|\psi|^2 \sim 1$ , the phase and amplitude relax at different rates. The correction due to inelastic electron-phonon scattering results in a different relaxation time of order parameter  $\psi$ , characterized by  $C^2 = 2\tau_{\text{in}}\Delta_0/(\hbar|\psi_0|^2)$ , where  $\Delta_0$  and  $\psi_0$  are values of the BCS gap and GL function at given temperature in the absence of currents.  $\tau_{\text{in}}$  is the inelastic electron-phonon scattering time. Since in pure superconductors  $\tau_{\text{in}}\Delta_0 \gg \hbar$ , the correction  $C^2|\psi|^2$  can be large under realistic conditions. We use this relaxation rate in the numerical example. Close to the critical line this correction vanishes and one can use a simpler theory corresponding to the limit  $C^2|\psi|^2 \rightarrow 0$  of Eq. (2).

Our major concern will be the contribution of the normal current through the  $\mathbf{J}_N$  term. In Eq. (2) the kinetic energy depends on the difference between the velocity of the condensate

$$\mathbf{v}_S = \frac{1}{m^*} \left( \hbar\nabla\chi - \frac{e^*}{c}\mathbf{A} \right), \quad (3)$$

where  $\chi$  is the phase of the superconducting order parameter  $\psi = |\psi|e^{i\chi}$ , and the mean velocity of normal electrons

$$\mathbf{v}_N = \frac{1}{en}\mathbf{J}_N. \quad (4)$$

The first term of Eq. (2) is thus the kinetic energy price which must be paid by a pair of normal electrons in order to join the condensate in the reference frame floating with normal electrons. To distinguish the theory based on the velocity difference from the standard TDGL theory, we refer to

the theory described by Eq. (2) as the *floating-kernel approximation*.<sup>13</sup>

### B. Two-fluid picture of current

The derivative of the kinetic energy with respect to vector potential  $\mathbf{A}$  defines the current operator. The correction to the normal current thus also appears in the supercurrent

$$\begin{aligned} \mathbf{J}_S &= \frac{e^*}{m^*} \text{Re} \left[ \bar{\psi} \left( -i\hbar\nabla - \frac{e^*}{c}\mathbf{A} - \frac{m^*}{en}\mathbf{J}_N \right) \psi \right] \\ &= e^*n_S(\mathbf{v}_S - \mathbf{v}_N), \end{aligned} \quad (5)$$

with  $n_S = |\psi|^2$  being the density of Cooper pairs or the condensate density. This supercurrent depends on the relative velocity of the condensate with respect to the normal background since according to Ohm's law (1) all electrons move with the normal velocity  $\mathbf{v}_N$ .

One can leave the picture of relative motion and instead rearrange the total current in the spirit of the two-fluid model:

$$\begin{aligned} \mathbf{J} &= \mathbf{J}_S + \mathbf{J}_N = e^*n_S(\mathbf{v}_S - \mathbf{v}_N) + en\mathbf{v}_N \\ &= e^*n_S\mathbf{v}_S + (en - e^*n_S)\mathbf{v}_N \\ &= \frac{e^*}{m^*} \text{Re} \left[ \bar{\psi} \left( -i\hbar\nabla - \frac{e^*}{c}\mathbf{A} \right) \psi \right] + \mathbf{J}_N \left( 1 - \frac{2|\psi|^2}{n} \right). \end{aligned} \quad (6)$$

In this rearrangement the supercurrent has the condensate velocity  $\mathbf{v}_S$ . The correction term becomes a part of the normal current, where it reduces the density of electrons to the fraction of normal electrons.

The necessity to reduce the normal current to the normal fraction follows from the longitudinal  $f$ -sum rule. In the Appendix we show that in order to achieve a consistent theory formulated via free energy, the reduced normal current must be accompanied by changes in the free energy which lead to the floating-kernel approximation.

### C. Scalar and vector potential

Let us close the set of equations. Potentials  $\mathbf{A}$  and  $\phi$  yield the electric field<sup>16</sup>

$$\mathbf{E}' = -\frac{1}{c}\frac{\partial\mathbf{A}}{\partial t} - \nabla\phi. \quad (7)$$

In some applications one should keep in mind that  $\phi$  is to be interpreted as a local electrochemical potential, not the electrostatic potential. The vector  $\mathbf{E}'$  is thus the driving force per electron rather than the Maxwell electric field. Following the notation of Josephson we indicate this distinction with a prime, but as is usual in the theory of superconductivity we simply refer to  $\mathbf{E}'$  as the electric field.

Although the system has nonzero scalar potential, deviations from charge neutrality are so small that one may neglect them, using the continuity equation in its stationary form  $\nabla \cdot \mathbf{J} = 0$ . Substituting Eq. (7) into the normal current from Eq. (1),  $\mathbf{J} = \mathbf{J}_S + \mathbf{J}_N$ , leads to the usual condition for the potential

$$\sigma_N \nabla^2 \phi = \nabla \cdot \mathbf{J}_S. \quad (8)$$

We have used  $\nabla \cdot \mathbf{A} = 0$  and assumed a homogeneous sample  $\nabla \sigma_N = 0$ . To evaluate the vector potential we need the

Maxwell equation

$$\nabla^2 \mathbf{A} = -\mu_0(\mathbf{J}_S + \mathbf{J}_N) \quad (9)$$

which is also in the stationary approximation to be consistent with the continuity equation. Thus, the set of equations (1), (2), (5), and (7)–(9) describe the dynamics of the system.

### III. TRANSIENT NATURE OF THE CURRENT-CURRENT INTERACTION

An overlap of the normal current and supercurrent appears at the conversion layer at the junction of the superconductor to a normal lead. Similarly, there is such an overlap at phase-slip centers in superconducting wires or at phase-slip lines in films. In this section we show that the floating-kernel correction is purely transient and contributes only if the electric and magnetic field change in time. The floating-kernel correction thus does not contribute at the conversion layer and at phase slip centers. In contrast, in the next section we will demonstrate via numerical simulation that the floating-kernel corrections are appreciable at the phase-slip lines which are formed by fast-moving kinematic vortices.

#### A. Effective vector and scalar potentials

The floating-kernel TDGL can be converted to the form of the normal TDGL by writing in terms of effective vector and scalar potentials  $\mathbf{A}_{\text{eff}}$  and  $\phi_{\text{eff}}$ . These effective potentials are associated with superconducting electrons, while  $\phi$  and  $\mathbf{A}$  are associated with normal electrons.

The normal current enters the floating-kernel approximation in two ways, appearing in the kinetic energy of Eq. (2) and also in the supercurrent (3). In each case  $\mathbf{J}_N$  and  $\mathbf{A}$  appear in the same combination, which can be replaced by a vector field

$$\mathbf{A}_{\text{fk}} = \mathbf{A} + \frac{m^*c}{2e^2n}\mathbf{J}_N. \quad (10)$$

It is advantageous to describe the vector and scalar potentials in a symmetrical way. We express the normal current (1) via potentials

$$\mathbf{J}_N = -\sigma_N \frac{1}{c} \frac{\partial \mathbf{A}}{\partial t} - \sigma_N \nabla \phi \quad (11)$$

so that

$$\mathbf{A}_{\text{fk}} = \mathbf{A} - \tau \frac{\partial \mathbf{A}}{\partial t} - c\tau \nabla \phi \quad (12)$$

with the characteristic time

$$\tau = \frac{m^*\sigma_N}{2e^2n}. \quad (13)$$

By substitution

$$\psi = e^{-ie^*\tau\phi/\hbar} \tilde{\psi}$$

and for a homogeneous sample with  $\nabla\tau = 0$ , the GL equation (2) assumes the form

$$\begin{aligned} & \frac{1}{2m^*} \left( -i\hbar\nabla - \frac{e^*}{c} \mathbf{A}_{\text{eff}} \right)^2 \tilde{\psi} + \alpha\tilde{\psi} + \beta|\tilde{\psi}|^2\tilde{\psi} \\ & = -\frac{\Gamma}{\sqrt{1+\gamma^2|\tilde{\psi}|^2}} \left( \frac{\partial}{\partial t} + \frac{i}{\hbar} e^* \phi_{\text{eff}} + \frac{\gamma^2}{2} \frac{\partial |\tilde{\psi}|^2}{\partial t} \right) \tilde{\psi} \end{aligned} \quad (14)$$

with effective potentials

$$\phi_{\text{eff}} = \phi - \tau \frac{\partial \phi}{\partial t}, \quad (15)$$

$$\mathbf{A}_{\text{eff}} = \mathbf{A} - \tau \frac{\partial \mathbf{A}}{\partial t}. \quad (16)$$

The supercurrent (5) reads

$$\mathbf{J}_S = \frac{e^*}{m^*} \text{Re} \left[ \tilde{\psi} \left( -i\hbar\nabla - \frac{e^*}{c} \mathbf{A}_{\text{eff}} \right) \tilde{\psi} \right] \quad (17)$$

while other equations of the TDGL theory need not be rewritten since they depend only on the amplitude  $|\psi|^2 = |\tilde{\psi}|^2$ .

The above formulation makes it clear that the system behaves as if the normal electrons are driven by potentials  $\phi$  and  $\mathbf{A}$  while the superconducting electrons experience effective potentials  $\phi_{\text{eff}}$  and  $\mathbf{A}_{\text{eff}}$ .

#### B. Effective electric and magnetic fields

Action of the above effective potentials can be expressed via effective magnetic and electric fields. The transverse component of the normal current acts on the condensate via an effective magnetic field

$$\mathbf{B}_{\text{eff}} = \nabla \times \mathbf{A}_{\text{eff}} = \mathbf{B} - \tau \frac{\partial \mathbf{B}}{\partial t}. \quad (18)$$

The time variation of the normal current acts on the condensate via an effective electric field

$$\mathbf{E}'_{\text{eff}} = -\frac{1}{c} \frac{\partial}{\partial t} \mathbf{A}_{\text{eff}} - \nabla \phi_{\text{eff}} = \mathbf{E}' - \tau \frac{\partial \mathbf{E}'}{\partial t}. \quad (19)$$

In both effective fields the correction term vanishes in the stationary limit. The corrections following from the floating-kernel picture might thus become important in transient regimes or in systems driven by oscillating fields. The ac response of the Abrikosov vortex lattice has been discussed in Ref. 13. Here we focus on vortices driven by a steady supercurrent.

### IV. NUMERICAL SIMULATIONS WITHIN THE TDGL THEORY

Subjected to a dc transport current, superconducting vortices start moving under the action of the Lorentz force, leading to energy dissipation in the system.<sup>17</sup> The mechanisms for the dissipation are known to be<sup>18</sup> the normal currents flowing in the vortex cores,<sup>19</sup> relaxation of the order parameter,<sup>20</sup> and the slow diffusion mechanism of relaxation of the order parameter caused by the anomalous term in the time-dependent microscopic theory.<sup>21</sup> At larger values of the external current, a nonequilibrium distribution of the quasiparticles takes place due to the finite relaxation time. As a result, the superconducting condensate is strongly reduced behind the vortex core, whereas it is enhanced in front of the vortex core. Such a deformation of the vortex core results in anisotropic interactions between the vortices leading to rearrangement of the triangular Abrikosov lattice to a set of parallel vortex rows with suppressed order parameter, similar to phase-slip lines.<sup>22</sup> Along these lines vortices move with velocities exceeding by orders of magnitude typical velocities of Abrikosov vortices in the flux flow regime.<sup>3,4</sup>

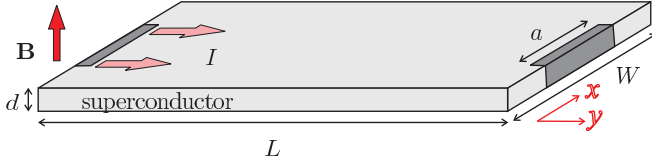


FIG. 1. (Color online) The model system: A superconducting strip of length  $L$ , width  $w$ , and thickness  $d$  in the presence of perpendicular applied field  $B$  and dc current  $I$ , applied through normal-metal contacts of size  $a$ . The output voltage is measured at a small distance away from these leads.

In this regime we expect significant contribution of floating-kernel corrections due to the following. First, near the fast-moving vortices time derivatives of the magnetic and electric fields are large so that the effective fields  $\mathbf{B}_{\text{eff}}$  and  $\mathbf{E}_{\text{eff}}$  can differ appreciably from the static fields. Second, there are large normal currents across the phase-slip line due to the suppressed superconductivity.

Since it is impossible to solve the highly nonlinear TDGL equations in such a nonequilibrium state<sup>23</sup> even in the one-dimensional case (see, e.g., Ref. 24), here we demonstrate the effect of the floating-kernel corrections due to the normal current and supercurrent interaction via numerical simulation. As an example we consider a superconducting strip with length  $L$ , thickness  $d \ll \xi, \lambda$ , and width  $w \ll \Lambda = 2\lambda/d^2$  in the presence of a transport current (applied through the normal contacts of size  $a$ ) and a perpendicular magnetic field  $B$  (see Fig. 1). Under this consideration one can neglect the back reaction of the current on the magnetic field and assume a constant homogenous magnetic field, so  $\mathbf{B}_{\text{eff}} = \mathbf{B}$ . Therefore, we neglect the floating-kernel corrections to the vector potential, and write  $\mathbf{A}_{\text{eff}} = \mathbf{A}$ . The effect of the normal current on the dynamics of the condensate will be taken into account through the effective scalar potential  $\phi_{\text{eff}}$ .

To understand the dynamical properties of the system we use the TDGL equation in dimensionless form

$$(\nabla' - i\mathbf{A}')^2 \psi' + (1 - T - |\psi'|^2) \psi' = \frac{u}{\sqrt{1 + \gamma^2 |\psi'|^2}} \left( \frac{\partial}{\partial t'} + i\phi'_{\text{eff}} + \frac{\gamma^2}{2} \frac{\partial |\psi'|^2}{\partial t'} \right) \psi', \quad (20)$$

which is coupled to the equation for the scalar potential

$$\nabla'^2 \phi' = \nabla' \cdot \mathbf{J}'_S, \quad (21)$$

where  $\mathbf{J}'_S = \text{Re}[\tilde{\psi}'(-i\nabla' - \mathbf{A}')\psi']$  is the supercurrent density. Here the order parameter  $\psi' = \tilde{\psi}/\psi_0$  is scaled with the GL value  $\psi_0^2 = -\alpha/\beta$ , temperature is in units of  $T_c$ , distance  $x' = x/\xi$  is scaled to the GL coherence length  $\xi^2 = -\hbar^2/2m^*\alpha$ , and the vector potential  $\mathbf{A}' = (e^*\xi/c\hbar)\mathbf{A}$  is in units of  $e^*\xi/c\hbar$ . The time  $t' = tu/\tau_{\text{GL}}$  is scaled with the GL time  $\tau_{\text{GL}} = -\Gamma/\alpha = \pi\hbar/8k_B(T_c - T)$  and the scalar effective potential scales with the inverse time  $\phi'_{\text{eff}} = (e^*\tau_{\text{GL}}/\hbar u)\phi_{\text{eff}}$ . We note that the scalar potential  $\phi'$  in Eq. (21) is in the same units  $\phi_0 = \hbar u/e^*\tau_{\text{GL}}$  as  $\phi'_{\text{eff}}$ . The current density is scaled as  $\mathbf{J}'_S = (m^*\xi/e^*\hbar\psi_0^2)\mathbf{J}_S$ . The amplitude-relaxation rate reads as  $\gamma = C\psi_0$  and the phase-relaxation rate  $u$  is defined as  $u = \pi\hbar/4k_B T_c \tau$ , which renders Eq. (21) free of numerical factors. In these units, the

effective potential relates to the true one as

$$\phi'_{\text{eff}} = \phi' - 2 \left( 1 - \frac{T}{T_c} \right) \frac{\partial}{\partial t'} \phi'. \quad (22)$$

Using the normal-state resistivity  $1/\sigma_N = \rho_N = 18.7 \mu\Omega \text{ cm}$ , zero temperature coherence length  $\xi(0) = 10 \text{ nm}$ , and penetration depth  $\lambda(0) = 200 \text{ nm}$ , which are typical for Nb thin films,<sup>25</sup> one can obtain  $t_{\text{GL}} \approx 2.69 \text{ ps}$  and  $\phi_0 \approx 0.12 \text{ mV}$  near  $T_c$ .

Following the numerical approach given in Ref. 26, we solve Eqs. (20) and (21) on a uniform Cartesian space grid, using the standard Euler iterative method for Eq. (20) and the successive over-relaxation method for Eq. (21). We use superconducting-vacuum boundary conditions  $(\nabla - i\mathbf{A})\psi|_n = 0$  and  $\nabla\phi|_n = 0$  at all sample boundaries, except at the current contacts where we use  $\psi = 0$  and  $\nabla\phi|_n = -j$ , with  $j$  being the applied current density. Assuming that  $w \ll \Lambda = 2\lambda/d^2$  we neglect the demagnetization effects and choose  $\mathbf{A} = (-By/2, Bx/2)$ . The material parameters  $u$  and  $\gamma$  are chosen as  $u = 5.79$  and  $\gamma = 10$ , which are found within the microscopic BCS theory for superconductors with weak depairing.<sup>15</sup> For a given value of the external current, we have conducted simulations for  $t_{\text{max}} = 10000\tau_{\text{GL}}$  and the voltage is averaged for the period  $\Delta t = t_{\text{max}}/2$ .

We study the time-averaged voltage versus current ( $I$ - $V$ ) characteristics by applying a constant current through the sample at a constant magnetic field. As a representative example we consider a superconducting strip with length  $L = 80\xi(0)$  and width  $w = 40\xi(0)$ , the  $I$ - $V$  curves of which are shown in Fig. 2 for different values of the applied magnetic field  $B$  at  $T = 0.75T_c$  with and without the floating-kernel corrections. At zero magnetic field (black curves) the system is in the fully superconducting state for the current density below  $j_{c2} = 0.35j_0$ , which is smaller than the GL depairing current density  $j_{\text{GL}} = 0.385j_0$ . When the critical current is reached, the system transits into the normal state. The effect of the floating-kernel correction is negligibly small at zero magnetic field (see lower inset in the main panel of Fig. 2). Vortices penetrate the sample with applying external magnetic field: For  $B = 0.1B_{c2}$  (red curve in Fig. 2) four vortices enter the sample at zero applied current. These vortices are displaced by small applied current (see panel 1). The vortices are set into motion by increasing the applied drive leading to a monotonic increase of output voltage (before point 2 the  $I$ - $V$  curve). First and second columns in panel 2 show the snapshots of those moving Abrikosov vortices in the two regimes. As we expected, the effect of the floating-kernel correction is not very pronounced in this slowly moving regime—the actual positions of the vortices are almost the same in the two approximations.

Third column of panel 2 in Fig. 2 shows a snapshot of the actual value of the floating correction to the scalar potential  $\delta = \tau \frac{\partial \phi}{\partial t}$ . Two main features can be highlighted in this plot: First, the contribution due to normal contacts, where the dissipative normal current is converted into dissipation-free supercurrent over a distance of a few times  $\xi$  via Andreev reflection,<sup>27</sup> is negligibly small. The second feature is that the floating-kernel corrections near the vortex core far from the surface have quadrupole symmetry. This can be understood from the Bardeen-Stephen picture<sup>19</sup> of the moving vortex; a vortex moving in the vertical direction creates an electric field which



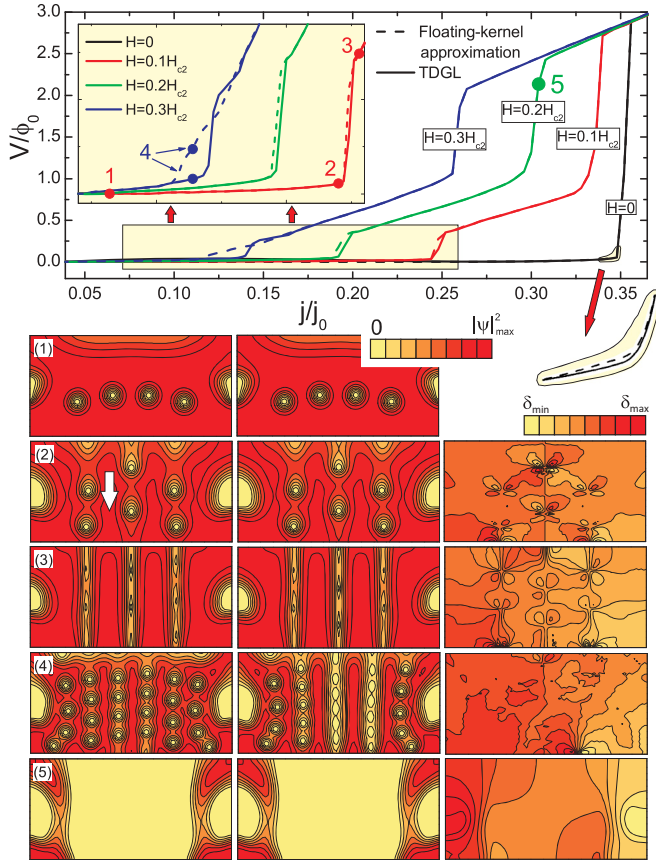


FIG. 2. (Color online)  $I$ - $V$  characteristics of the sample with dimensions  $L = 80\xi(0)$ ,  $w = 40\xi(0)$ , and  $a = 8\xi(0)$  at temperature  $T = 0.75T_c$  for different values of the applied magnetic field  $B$  without (solid curves) and with (dashed curves) the floating-kernel approximation to the electrostatic potential. Insets show the low voltage part of the  $I$ - $V$  curve. Panels 1–5 shows the snapshots of the Cooper pair density without (first column) and with (second column) the floating-kernel correction at the field and current values indicated on the  $I$ - $V$  curves. The third column shows the floating-kernel correction to the electrostatic potential  $\delta = \tau \frac{\partial \phi}{\partial t}$ . The white arrow in panel 2 shows the direction of vortex motion.

drives the normal current through its core in the horizontal direction. The corresponding scalar potential is thus a dipole with horizontal orientation. The time derivative of this potential due to its vertical translation exhibits the quadrupole symmetry.

With further increasing the applied current the system transits into a resistive state with a finite voltage jump (point 3 in Fig. 2) characterized by fast-moving kinematic vortices. First and second columns in panel 3 of Fig. 2 show the snapshots of such kinematic vortices in this regime. Although both approximations give the same number of phase-slip lines, the actual position of the kinematic vortices is different in two regimes. Such kinematic vortices lead to time-periodic voltage oscillations across the sample, the frequency of which can range up to the sub-THz regime (see Fig. 9 in Ref. 4). The third column in panel 3 of Fig. 2 shows a snapshot of the correction to the electrostatic potential in the phase-slip state  $\delta$ . Although  $\delta$  shows the same behavior as in the case of slow moving Abrikosov vortices, the value of  $\delta$  is two orders of

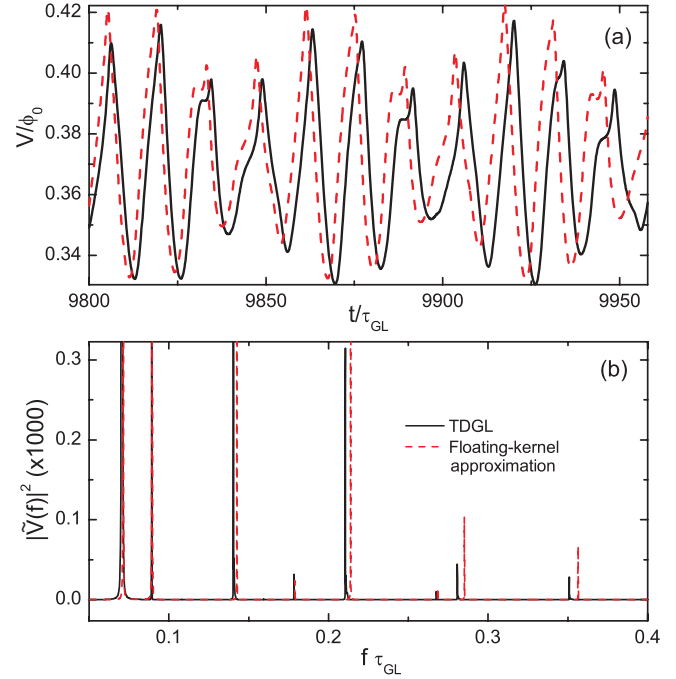


FIG. 3. (Color online) (a) Time evolution of the voltage of the sample in Fig. 2 for  $j = 0.256j_0$  and  $B = 0.1B_{c2}$  (indicated by point 3 on the  $I$ - $V$  curve in Fig. 2) without (solid black curve) and with (dashed red curve) the floating-kernel correction. (b) The Fourier power spectrum of  $V(t)$ .

magnitude larger in the phase-slip state being still only few percent of the steady potential due to the finite conductivity.

To see clearly the effect of the floating-kernel correction to the voltage response of the system to the external field, we plotted in Fig. 3(a) the time evolution of the voltage across the sample in the phase-slip regime. The  $V(T)$  curves in both cases show clear oscillations with maxima corresponding to penetration or expulsion of kinematic vortices. The effect of the floating correction to the amplitude of the oscillations are clearly seen in this figure. To see how the period of these oscillations are affected by the correction, we conducted Fourier analysis of the voltage curves, which is plotted in Fig. 3(b). The Fourier power spectrum shows that the frequency of the oscillations increases when the correction to the electrostatic potential is taken into account. As a result, the critical current for the transition into this resistive state becomes smaller when we take the floating-kernel correction into account (see red and green curves in Fig. 2).

The effect of the floating-kernel approximation becomes more pronounced at higher magnetic field, resulting in significant reduction of the resistive state transition current (see solid and dashed blue curves in the  $I$ - $V$  in Fig. 2). The reason is the increased number of vortices in the system, each of them contributing to the correction to the effective electric potential due to the normal electrons in their core (see panel 4 in Fig. 2). Figure 4 shows the voltage vs time curves of the sample at  $B = 0.3B_{c2}$  for the current  $j = 0.128j_0$ . At this value of the current the floating-kernel correction brings the system into the resistive state [higher frequency of the  $V(t)$  oscillations], whereas the system is in the slow moving vortices state in the standard TDGL approach.

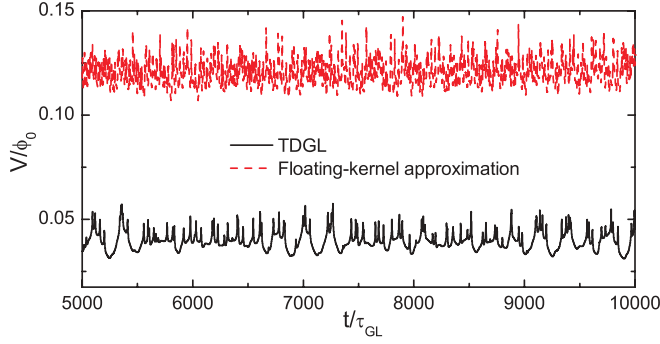


FIG. 4. (Color online) The same as in Fig. 3 but for the applied current density  $j = 0.128j_0$  and magnetic field  $B = 0.3B_{c2}$  (indicated by point 4 on the  $I$ - $V$  curve in Fig. 2).

The resistive state at higher fields is usually characterized by the coexistence of slow moving Abrikosov and fast moving kinematic vortices, as shown in the second column of panel 4 in Fig. 2. The formation of kinematic vortices reduces the number of vortex channels in the system (compare first and second columns in panel 4).<sup>22</sup> However, the total number of vortices inside the sample at a time remains the same. Another feature of the floating correction to the scalar potential  $\delta$  is seen from its contour plot in the latter state (third column in panel 4): The strongest contribution to  $\delta$  comes from the vortices at the sample edge. This is due to the fact that the velocity of vortices near the edges is much larger than the speed of vortices in the interior of sample.<sup>3,4</sup> As we mentioned above, the correction to the Abrikosov vortices is much smaller (due to their slower motion) and it is invisible in the scale of the figure.

The last jump in the  $I$ - $V$  curves before the system transits into the normal state (see point 5 in Fig. 2) is characterized by the collapse of the superconducting condensate in the middle of the sample and by the remnant superconductivity near the corners (see panel 5 in Fig. 2). Since there are no kinematic vortices in this regime and eventual floating-kernel corrections are negligibly small, both the critical current and the value of the voltage are the same in both the approximations. The correction to the electrostatic potential due the conversion of normal current into supercurrent near the normal contacts (see third column in panel 5 of Fig. 2) turns out to be small to influence the critical current of the sample.

## V. CONCLUSIONS

Within the floating-kernel approximation we studied the effect of the normal current on dynamics of the superconducting condensate in type-II superconductors. We showed that this effect is of transient nature and contributes only when the system evolves. The most pronounced effects were found for kinematic vortices which move much faster than isolated Abrikosov vortices. Particularly strong corrections were found near sample edges where kinematic vortices are accelerated, increasing their speed nearly by an order of magnitude. We found that both the resistive state transition critical current and voltage vs time characteristics of the sample is affected by the floating-kernel correction to the scalar potential.

## ACKNOWLEDGMENTS

The authors are grateful to Alex Gurevich and Tom Lemberger who brought the longitudinal  $f$ -sum rule to our attention. This work was supported by Grants GAČR P204/10/0687 and P204/11/0015. We also acknowledge the support from the Flemish Science Foundation (FWO-VI) and the Belgian Science Policy (IAP). G.R.B. acknowledges individual support from FWO-VI. P.-J.L. acknowledges support from Old Dominion University. P.M. acknowledges support through UA research index SR-614-1203.

## APPENDIX: FREQUENCY SUM RULE

The conductivity must satisfy the frequency sum rule<sup>28,29</sup>

$$\frac{2}{\pi} \int_0^\infty d\omega \text{Re}\sigma(\omega, \mathbf{k}) = \frac{ne^2}{m}, \quad (\text{A1})$$

where  $e$ ,  $m$ , and  $n$  are charge, mass, and density of electrons. To satisfy this sum rule, a modification of the TDGL theory in the spirit of the two-fluid theory is necessary. Here we show that this two-fluid correction implies the floating-kernel approximation discussed in Sec. II.

### 1. Sum-rule violation in the TDGL theory

First we show that the standard TDGL theory leads to conductivity which violates the sum rule (A1). In the standard TDGL theory the total current is expressed as a sum of the supercurrent and the normal current,

$$\mathbf{J}_{\text{TDGL}} = \mathbf{J}_{\text{GL}} + \mathbf{J}_N. \quad (\text{A2})$$

Neglecting the Hall effect, both currents are parallel to the electric field and the conductivity is a scalar given by the ratio  $\sigma = \mathbf{J}/\mathbf{E}'$ . It thus has two corresponding parts

$$\sigma_{\text{TDGL}} = \sigma_{\text{GL}} + \sigma_N. \quad (\text{A3})$$

The sum rule (A1) is satisfied in the normal state

$$\frac{2}{\pi} \int_0^\infty d\omega \text{Re}\sigma_N(\omega, \mathbf{k}) = \frac{ne^2}{m}. \quad (\text{A4})$$

The superconducting component of mean Cooperon density  $\bar{n}_S$ , mass  $m^*$ , and charge  $e^*$  appear in an analogous sum over frequencies

$$\frac{2}{\pi} \int_0^\infty d\omega \text{Re}\sigma_{\text{GL}}(\omega, \mathbf{k}) = \frac{\bar{n}_S e^{*2}}{m^*}. \quad (\text{A5})$$

The total sum rule (A1) for  $\sigma_{\text{TDGL}}$  is therefore violated.

### 2. Two-fluid correction

Assuming that formation of condensate depletes the supply of normal electrons  $n_N = n - 2\bar{n}_S$ , the normal conductivity ought to be correspondingly lowered,

$$\sigma = \sigma_{\text{GL}} + \left(1 - \frac{2\bar{n}_S}{n}\right) \sigma_N. \quad (\text{A6})$$

The sum over frequencies on the left-hand side of (A1) is then

$$\frac{2}{\pi} \int_0^\infty d\omega \text{Re}\sigma(\omega, \mathbf{k}) = \frac{\bar{n}_S e^{*2}}{m^*} + \left(1 - \frac{2\bar{n}_S}{n}\right) \frac{ne^2}{m}. \quad (\text{A7})$$

The sum rule (A7) corresponds to the sum rule valid in the Meissner state, when a part of the weight due to superconducting electrons is covered by the singular term in form of the Dirac  $\delta$  function.<sup>29-31</sup> Avoiding the  $\delta$  function one arrives at the sum rule<sup>29</sup>

$$\frac{2}{\pi} \int_{0^+}^{\infty} d\omega \text{Re}\sigma(\omega, \mathbf{k}) = \left(1 - \frac{2\bar{n}_S}{n}\right) \frac{ne^2}{m}. \quad (\text{A8})$$

Here we assume similar structure for the mixed state. The only difference is that in the presence of vortices the conductivity  $\sigma_{\text{GL}}$  of superconducting electrons is finite even at zero frequency. Its frequency dependence is not a  $\delta$  function but has a Drude form.

In the pure limit,  $m^* = 2m$ , the sum rule (A1) is satisfied. As one can see, the sum rule (A1) is violated in the dirty limit when  $m^* \neq 2m$ . This corresponds to limitations of the theory used to derive the floating-kernel approximation. The derivation of Ref. 7 is based on the Kadanoff-Baym ansatz with the spectral function approximated by the Dirac  $\delta$  function, therefore the renormalization of the Cooper-pair mass due to finite mean free path is not included in this approach. Briefly, the floating-kernel approximation is justified only in the pure limit.

### 3. Interaction of normal current with condensate

We note that the floating-kernel approximation discussed in Sec. II leads to the conductivity (A6); see the current (6). Here we approach the problem from the opposite direction; starting from the conductivity (A6) we arrive at the floating-kernel approximation.

Let us require that the set of TDGL equations must follow from the effective free energy:<sup>32</sup>

$$\Gamma \left( \frac{\partial}{\partial t} + ie^*\phi \right) \psi = -\frac{\delta \mathcal{F}}{\delta \bar{\psi}}, \quad (\text{A9})$$

$$\mathbf{J} = -\frac{\delta \mathcal{F}}{\delta \mathbf{A}}. \quad (\text{A10})$$

Since our focus is on the spatial gradients, we neglect the nonlinear relaxation of Kramer and Watts-Tobin. Indeed, the relaxation on the left-hand side of Eq. (A9) results from sending  $C \rightarrow 0$  in Eq. (2)

In Eqs. (A9) and (A10) the GL function  $\psi$  is normalized to the Cooperon density as  $n_S = |\psi|^2$  and the sum rule uses the value averaged over space  $\bar{n}_S = \langle |\psi|^2 \rangle$ . We assume that the free energy can be additively decomposed into superconducting and normal parts,  $\mathcal{F} = \mathcal{F}_N + \mathcal{F}_S$ , where the normal part is the same as in the normal state and therefore

$$\mathbf{J}_N = -\frac{\delta \mathcal{F}_N}{\delta \mathbf{A}}. \quad (\text{A11})$$

The GL function thus enters the superconducting part only,

$$\frac{\delta \mathcal{F}_N}{\delta \bar{\psi}} = 0. \quad (\text{A12})$$

In the TDGL theory the supercurrent reads

$$\mathbf{J}_{\text{GL}} = \frac{e^*}{m^*} \text{Re} \left[ \bar{\psi} \left( -i\hbar \nabla - \frac{e^*}{c} \mathbf{A} \right) \psi \right]. \quad (\text{A13})$$

Since the vector potential  $\mathbf{A}$  appears exclusively via the covariant spatial gradient seen here, this expression implies that in the TDGL free energy the kinetic energy takes the familiar form  $(1/2m^*)|[-i\hbar \nabla - (e^*/c)\mathbf{A}]\psi|^2$ .

We have seen that the current (A13) with the normal current added violates the frequency sum rule. Now we derive the kinetic energy assuming that current includes the two-fluid correction. According to the two-fluid conductivity (A6), the total current reads

$$\begin{aligned} \mathbf{J} &= \sigma_{\text{GL}} \mathbf{E}' + \left(1 - \frac{2n_S}{n}\right) \sigma_N \mathbf{E}' \\ &= \mathbf{J}_{\text{GL}} - \frac{2n_S}{n} \mathbf{J}_N + \mathbf{J}_N \\ &= \frac{e^*}{m^*} \text{Re} \bar{\psi} \left( -i\hbar \nabla - \frac{e^*}{c} \mathbf{A} - \frac{m^*}{en} \mathbf{J}_N \right) \psi + \mathbf{J}_N. \end{aligned} \quad (\text{A14})$$

We have in the supercurrent included the correction term because it is proportional to the condensate density. According to Eqs. (A10) and (A12) it thus cannot result from the variation of the normal free energy  $\mathcal{F}_N$ .

From Eqs. (A10), (A11), and (A14)

$$\frac{\delta \mathcal{F}_S}{\delta \mathbf{A}} = -\frac{e^*}{m^*} \text{Re} \bar{\psi} \left( -i\hbar \nabla - \frac{e^*}{c} \mathbf{A} - \frac{m^*}{en} \mathbf{J}_N \right) \psi. \quad (\text{A15})$$

Integrating relation (A15) over the vector potential one finds the superconducting free energy

$$\begin{aligned} \mathcal{F}_S &= \frac{1}{2m^*} \left| \left( -i\hbar \nabla - \frac{e^*}{c} \mathbf{A} - \frac{m^*}{en} \mathbf{J}_N \right) \psi \right|^2 \\ &\quad + \alpha |\psi|^2 + \frac{1}{2} \beta |\psi|^4. \end{aligned} \quad (\text{A16})$$

Of course, the integration provides only the kinetic energy which has to be rearranged with integration by parts into the square of covariant gradients. The terms independent of  $\mathbf{A}$  represent an initial condition of the integral and are taken from the standard GL theory.

With free energy (A16), Eq. (A9) is identical to the floating-kernel approximation (2) in the  $C \rightarrow 0$  limit. It should be noted that derivation of Eq. (2) from microscopic theory was also extended to the linear terms in  $\mathbf{J}_N$ , therefore additional terms quadratic in the normal current might appear.

To summarize this Appendix, we have shown that the TDGL theory violates the longitudinal  $f$ -sum rule. To restore the sum rule the normal current must be reduced, corresponding to an interaction term between the normal current and the condensate. In this way one recovers the floating-kernel approximation from phenomenological arguments.

<sup>1</sup>B. Biehler, B. U. Runge, P. Leiderer, and R. G. Mints, *Phys. Rev. B* **72**, 024532 (2005).

<sup>2</sup>J. I. Vestgård, D. V. Shantsev, Y. M. Galperin, and T. H. Johansen, *Phys. Rev. B* **84**, 054537 (2011).

<sup>3</sup>A. Andronov, I. Gordion, V. Kurin, I. Nefedov, and I. Shereshevsky, *Physica C* **213**, 193 (1993).

<sup>4</sup>G. R. Berdiyrov, M. V. Milošević, and F. M. Peeters, *Phys. Rev. B* **79**, 184506 (2009).

- <sup>5</sup>E. Sardella, P. N. Lisboa Filho, C. C. de Souza Silva, L. R. Eulalio Cabral, and W. Aires Ortiz, *Phys. Rev. B* **80**, 012506 (2009).
- <sup>6</sup>D. Y. Vodolazov and F. M. Peeters, *Phys. Rev. B* **81**, 184521 (2010).
- <sup>7</sup>P. J. Lin and P. Lipavský, *Phys. Rev. B* **77**, 144505 (2008).
- <sup>8</sup>A. Schmid and G. Schön, *J. Low Temp. Phys.* **20**, 207 (1975).
- <sup>9</sup>L. Kramer and R. J. Watts-Tobin, *Phys. Rev. Lett.* **40**, 1041 (1978).
- <sup>10</sup>C. R. Hu, *Phys. Rev. B* **21**, 2775 (1980).
- <sup>11</sup>J. A. Pals, K. Weiss, P. M. Vanattekum, R. E. Horstman, and J. Wolter, *Phys. Rep.* **89**, 323 (1982).
- <sup>12</sup>D. J. Thouless, *Ann. Phys.* **10**, 553 (1960).
- <sup>13</sup>P. J. Lin and P. Lipavský, *Phys. Rev. B* **80**, 212506 (2009).
- <sup>14</sup>Y. Ikebe, R. Shimano, M. Ikeda, T. Fukumura, and M. Kawasaki, *Phys. Rev. B* **79**, 174525 (2009).
- <sup>15</sup>R. J. Watts-Tobin, Y. Krähenbühl, and L. Kramer, *J. Low Temp. Phys.* **42**, 459 (1981).
- <sup>16</sup>B. D. Josephson, *Phys. Lett.* **16**, 242 (1965).
- <sup>17</sup>Y. B. Kim, C. F. Hempstead, and A. R. Strnad, *Phys. Rev.* **139**, 1163 (1965).
- <sup>18</sup>S. J. Poon and K. M. Wong, *Phys. Rev. B* **27**, 6985 (1983).
- <sup>19</sup>J. Bardeen and M. J. Stephen, *Phys. Rev.* **140**, A1197 (1965).
- <sup>20</sup>M. Tinkham, *Phys. Rev. Lett.* **13**, 804 (1964).
- <sup>21</sup>L. P. Gor'kov and N. B. Kopnin, *Zh. Eksp. Teor. Fiz.* **64**, 356 (1973) [*Sov. Phys. JETP* **37**, 183 (1973)]; **65**, 396 (1973) [**38**, 195 (1974)].
- <sup>22</sup>D. Y. Vodolazov and F. M. Peeters, *Phys. Rev. B* **76**, 014521 (2007).
- <sup>23</sup>M. Machida and H. Kaburaki, *Phys. Rev. Lett.* **71**, 3206 (1993).
- <sup>24</sup>V. V. Baranov, A. G. Balanov, and V. V. Kabanov, *Phys. Rev. B* **84**, 094527 (2011).
- <sup>25</sup>A. I. Gubin, K. S. Il'in, S. A. Vitusevich, M. Siegel, and N. Klein, *Phys. Rev. B* **72**, 064503 (2005).
- <sup>26</sup>G. R. Berdiyurov, A. K. Elmurodov, F. M. Peeters, and D. Y. Vodolazov, *Phys. Rev. B* **79**, 174506 (2009).
- <sup>27</sup>A. F. Andreev, *Zh. Eksp. Teor. Fiz.* **46**, 1823 (1964) [*Sov. Phys. JETP* **19**, 1228 (1964)].
- <sup>28</sup>P. C. Martin and J. Schwinger, *Phys. Rev.* **115**, 1345 (1959).
- <sup>29</sup>D. N. Basov and T. Timusk, *Rev. Mod. Phys.* **77**, 721 (2005).
- <sup>30</sup>R. A. Ferrell and R. E. Glover, *Phys. Rev.* **109**, 1398 (1958).
- <sup>31</sup>M. Tinkham and R. A. Ferrell, *Phys. Rev. Lett.* **2**, 331 (1959).
- <sup>32</sup>I. J. R. Aitchison, P. Ao, D. J. Thouless, and X.-M. Zhu, *Phys. Rev. B* **51**, 6531 (1995).